Resonant quantum transport in semiconductor nanostructures

E. R. Racec* and Ulrich Wulf
Technische Universität Cottbus, Fakultät 1, Postfach 101344, D-03013 Cottbus, Germany
(Received 31 March 2001; published 30 August 2001)

We develop a theory of the conductance of a multichannel double barrier system in the case of decoupled channels. In the frame of the Landauer-Büttiker formalism we find two basic contributions to the conductance: first, a resonant one described by a Fano profile with a complex asymmetry parameter and second a noncoherent background which can be assumed as a constant in the case of small overlap of the conductance peaks. We establish a method to reconstruct the *S* matrix from the experimental conductance data.

DOI: 10.1103/PhysRevB.64.115318 PACS number(s): 73.40.Gk, 73.21.−b, 73.23.Ad

I. INTRODUCTION

In the recent years the study of line shapes in resonant transport through semiconductor nanostructures has attracted considerable attention. Of particular interest are asymmetric resonances and antiresonances. In Fano theory both line shapes result from a coherent interaction of the resonance with a given background.[1,2] To meet this condition usually a scenario is considered in which two transmission channels interfere: First, a resonant channel which is provided by a quasibound level, second, a background channel which is provided by a continuum of propagating states. In many studies the continuum of states is associated with a propagating mode in an electron wave guide.[3] The resonant channel can be established by a quasibound state in the binding potential of a donor impurity,[4] by the Γ-X-Γ channel in GaAs/AlAs/GaAs single-barrier structures[5] or by a resonantly coupled cavity.[6] An interesting variation of the latter case is the integration of the cavity in an Aharonov-Bohm ring.[7] A similar pattern as in Refs. 3–7 is followed in Ref. 8 analyzing magnetotransport across a quantum well. On the experimental side a first study of Fano profiles in transport was reported very recently in conductance measurements on a single-electron transistor.[9] The measured resonances show typical features of asymmetric and antiresonant Fano profiles. However, there remain serious open questions: First, in agreement with the standard explanation for Fano resonances there is a resonant part of the transmission which is well understood as a single-electron addition but no coherent background channel can be identified. Second, since there are minima in the conductance but no zeros an incoherent contribution to the conductance had to be assumed. As an alternative explanation a complex asymmetry parameter was proposed. Such a complex asymmetry parameter of the Fano distribution has been reported in a number of optical experiments.[10,11] The aim of this paper is to derive an analytical theory of transport resonances to discuss possible origins of the noncoherent contribution and of the complex asymmetry parameter.

We use the *S*-matrix description of coherent transport in which a Fano resonance is obtained from a pole of the *S* matrix in the complex energy plane of the standard form[2,12–14]

$$\tilde{\mathbf{S}}(E)=i\frac{\tilde{\mathbf{S}}(E_0)-\tilde{\mathbf{S}}_{\rm bg}}{e+i}+\tilde{\mathbf{S}}_{\rm bg}, \tag{1}$$

where $e=2(E-E_0)/\Gamma$. The first factor represents the resonant part of the transmission where the real numbers E_0 and Γ give position and width of the resonance. The second factor, $\tilde{\mathbf{S}}_{\rm bg}$, represents the nonresonant part.[15,16] For each matrix element of $\tilde{\mathbf{S}}$ it is seen from Eq. (1) that the resonant part undergoes a phase change of π when the energy passes the resonance. In general, this produces a change between constructive and destructive superposition of the resonant and the nonresonant part and an asymmetric line is obtained. In the standard approach the matrix $\tilde{\mathbf{S}}_{\rm bg}$ is chosen so that $\tilde{\mathbf{S}}(E)$ is unitary for *all* energies.[2,12–14] It follows that $\tilde{\mathbf{S}}_{\rm bg}$ has to be a unitary matrix (see Appendix D). Then a line shape $T(E)=T_{\rm bg}f(e), T_{\rm bg}=|(\tilde{\mathbf{S}}_{\rm bg})_{12}|^2$, results with the Fano function

$$f(e)=\frac{(e+q_r)^2}{e^2+1}, \tag{2}$$

where the asymmetry parameter q_r is real. Conflicting with the experiment the Fano function yields a zero in the conductance at $e=-q_r$.

Our starting point is a noninteracting model for one-dimensional transport through a quantum dot. The advantage of this model is that in difference to the approaches[2,12–14] it is possible to derive explicit expressions for the *S* matrix in Eq. (1) starting from the Schrödinger equation. In contrast to the situation in Refs. 3–7 there is only one (conserved) channel per contact for a given energy so that the usual picture to explain asymmetric lines which invokes coupling between two different channels does not apply. Nevertheless, we obtain Fano profiles in our model. To explain this, we first demonstrate in Sec. II that to each conductance peak a resonant channel can be associated which provides the resonant part of the conductance. The other channels yield a noncoherent contribution which for narrow resonances can be approximated as a constant.

In Sec. III we analyze the conductance contribution of the resonant channel and obtain Fano profiles with a complex asymmetry parameter. The coherent background component $\tilde{\mathbf{S}}_{\rm bg}$ of the *S* matrix which is necessary for an asymmetric line shape [Eq. (1)] is the natural consequence of the existence of other poles of the S-matrix in the complex energy plane which are different from the resonant pole. As illustrated in Ref. 17 these poles contribute in virtual (second order) processes to the transport. The imaginary part of the asymmetry

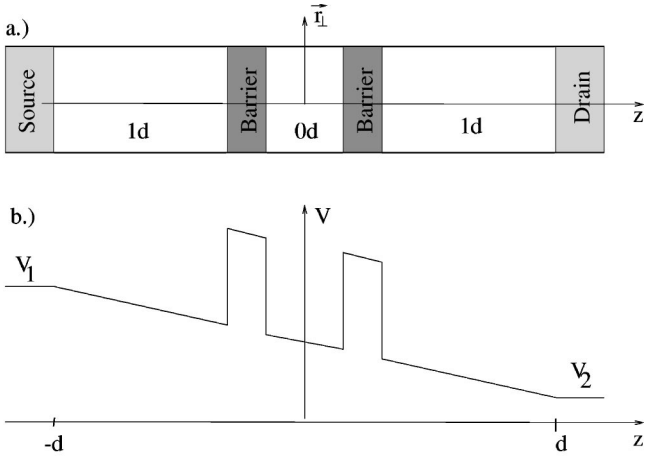

FIG. 1. (a) Schematic illustration of the system geometry; (b) z-dependent part of the potential.

parameter results from the following consideration: We obtain Eq. (1) for the S matrix by a linearization of the S matrix around the conductance maximum. Our description of the resonances therefore is correct in the center of the resonances, i.e., for $e \leqslant 1$. This is sufficient since if there is an overlap of the experimental resonances as in Ref. 9 a single pole approximation of the matrix as in Eq. (1) cannot be expected to be valid outside the center of the resonances. Therefore, in contrast to the standard approach which requires unitarity of $\tilde{\mathbf{S}}$ in the whole energy range [even where Eq. (1) cannot be expected to hold any more] our linearization yields unitarity of the S matrix only in linear order of e. Then, $\tilde{\mathbf{S}}_{\mathrm{bg}}$ does not have to be a unitary matrix and we gain one more free parameter for the line shape. We demonstrate that this parameter consists of the imaginary part of the asymmetry parameter which has to be introduced in Eq. (2). From numerical calculation we conclude that a complex asymmetry parameter is a general finding even for extremely narrow and strongly isolated resonances.

In Sec. IV we discuss our results on the background of the experiments in Ref. 9. Since the contacts in the experiments are two-dimensional there is the possibility of channel interaction which is not considered in our model. Nevertheless, we expect that the basic structure of our results carries over to the experimental geometry. It is then demonstrated that within certain limits it is possible to reconstruct from the experimental data the off-diagonal part of the S matrix as given in Eq. (1) up to a natural global phase.

II. THE MODEL

We consider an effectively one-dimensional system as depicted in Fig. 1. The electronic wave functions are the solutions to the Schrödinger equation

$$\left\{ -\frac{\hbar^2}{2m^*}\Delta + V(z) + V_\perp(\vec{r}_\perp) - E \right\} \mathbf{\Psi}(\vec{r}) = 0, \tag{3}$$

where the z-independent lateral confinement potential $V_\perp(\vec{r}_\perp)$ produces the one-dimensional character of the structure and $V(z)$ is a double barrier potential separating a quantum dot from the rest of the system. As usual we take $V(z)$ as constant in the contacts, $V(z<-d)=V_1$ for the source and $V(z>d)=V_2$ for the drain. The potential difference $V_{\mathrm{SD}} = V_1 - V_2$ results from an externally applied drain-source voltage. For the sake of simplicity the contacts are supposed to be identical.

Due to the separable form of the potential, the wave functions at the total energy E can be written as

$$\mathbf{\Psi}(\vec{r}) = \sum_\nu a_\nu(E)\,\psi(\epsilon^\nu, z)\Phi_\nu(\vec{r}_\perp), \tag{4}$$

with $\epsilon^\nu = E - E_\perp^\nu$ and the general expansion coefficients a_ν. The functions $\Phi_\nu(\vec{r}_\perp)$ and energies $E_\perp^\nu$ are the solutions to the eigenvalue problem

$$\left\{ -\frac{\hbar^2}{2m^*}\Delta_{\vec{r}_\perp} + V_\perp(\vec{r}_\perp) - E_\perp^\nu \right\} \Phi_\nu(\vec{r}_\perp) = 0. \tag{5}$$

We assume that $V_\perp(|\vec{r}_\perp| \to \infty) \to \infty$ so that the $\Phi_\nu(\vec{r}_\perp)$ can be chosen as a discrete orthonormal function system. The functions $\psi(\epsilon, z)$ are the solutions to the one-dimensional problem

$$\left\{ -\frac{\hbar^2}{2m^*}\frac{d^2}{dz^2} + V(z) - \epsilon \right\} \psi(\epsilon, z) = 0. \tag{6}$$

Because $V(z)$ is constant in the contacts we can write generally

$$\psi(\epsilon^\nu, z<-d) = \frac{1}{\sqrt{2\pi}}\{\psi_\nu^{\mathrm{in}}(-d)\exp[ik_{1\nu}(z+d)] + \psi_\nu^{\mathrm{out}}(-d)\exp[-ik_{1\nu}(z+d)]\} \tag{7}$$

and

$$\psi(\epsilon^\nu, z>d) = \frac{1}{\sqrt{2\pi}}\{\psi_\nu^{\mathrm{in}}(+d)\exp[-ik_{2\nu}(z-d)] + \psi_\nu^{\mathrm{out}}(+d)\exp[ik_{2\nu}(z-d)]\}, \tag{8}$$

with general expansion coefficients $\psi_\nu^{\mathrm{in/out}}(\pm d)$ and

$$k_{s\nu} = \sqrt{\frac{2m^*}{\hbar^2}(\epsilon^\nu - V_s)} \tag{9}$$

with $s=1,2$. Since we are interested in transport we only consider in Eq. (4) the radiating part of the spectrum with real wave vectors so that $\epsilon^\nu - V_m > 0$, where $V_m = \max(V_1, V_2)$ and ϵ^ν is the kinetic energy of the motion in the z direction. For a fixed energy E and fixed channel quantum number ν there are only two independent solutions of Eq. (6). Therefore the four coefficients $\psi_\nu^{\mathrm{in/out}}(\pm d)$ cannot be independent. In fact, defining the one-dimensional scattering area $z \in [-d, d]$ with the zero-dimensional surface $z = \pm d$ and using the S matrix of the one-dimensional problem Eq. (6) we obtain the condition

$$\psi_\nu^{\rm out}(z)=S(\epsilon^\nu,z,-d)\psi_\nu^{\rm in}(-d)+S(\epsilon^\nu,z,d)\psi_\nu^{\rm in}(d) \quad (10)$$

for $|z|\geqslant d$, i.e., outside the scattering area. Evaluation of Eq. (10) at $z=\pm d$ leads to the following 2×2-matrix equation:

$$\begin{pmatrix}\psi_\nu^{\rm out}(-d)\\ \psi_\nu^{\rm out}(+d)\end{pmatrix}=\begin{pmatrix}S(\epsilon^\nu,-d,-d) & S(\epsilon^\nu,-d,d)\\ S(\epsilon^\nu,d,-d) & S(\epsilon^\nu,d,d)\end{pmatrix}\begin{pmatrix}\psi_\nu^{\rm in}(-d)\\ \psi_\nu^{\rm in}(+d)\end{pmatrix}. \quad (11)$$

In view of the constraint (11) only the two ingoing components can be chosen independently. Taking $\psi_\nu^{\rm in}(-d)=1$ and $\psi_\nu^{\rm in}(d)=0$ yields the scattering state

$$\psi^{(1)}(\epsilon^\nu,z)=\frac{1}{\sqrt{2\pi}}\begin{cases} r_\nu^{(1)}\exp[-ik_{1\nu}(z+d)] & \\ \quad+\exp[ik_{1\nu}(z+d)], & z<-d,\\ t_\nu^{(1)}\exp[ik_{2\nu}(z-d)], & z>d.\end{cases} \quad (12)$$

This state corresponds to a particle incident from the source contact. Comparison with Eq. (11) yields $t_\nu^{(1)}=S(\epsilon^\nu,d,-d)$ and $r_\nu^{(1)}=S(\epsilon^\nu,-d,-d)$. Taking $\psi_\nu^{\rm in}(-d)=0$ and $\psi_\nu^{\rm in}(d)=1$ leads to

$$\psi^{(2)}(\epsilon^\nu,z)=\frac{1}{\sqrt{2\pi}}\begin{cases} t_\nu^{(2)}\exp[-ik_{1\nu}(z+d)], & z<-d,\\ r_\nu^{(2)}\exp[ik_{2\nu}(z-d)] & \\ \quad+\exp[-ik_{2\nu}(z-d)], & z>d\end{cases} \quad (13)$$

describing an incident wave coming from the drain contact. Here, $r_\nu^{(2)}=S(\epsilon^\nu,d,d)$ and $t_\nu^{(2)}=S(\epsilon^\nu,-d,d)$.

To calculate the current in the Landauer-Büttiker formalism,[18] the electrons can be thought of as two Fermi gasses: First, the electrons coming from the source contact. They occupy the single-particle scattering states $\psi^{(1)}(\epsilon,z)$ according to the Fermi-Dirac distribution function $f_{\rm FD}(E-\mu_1)$, where μ_1 is the chemical potential of the source contact. Second, the electrons coming from the drain contact with single-particle states $\psi^{(2)}(\epsilon,z)$ and with the chemical potential μ_2 of the drain contact. Summing up for all single-particle states the occupation factor times the expectation value of the current operator we obtain

$$I_z=\frac{2e}{h}\int dE[f_{\rm FD}(E-\mu_1)-f_{\rm FD}(E-\mu_2)]$$

$$\times\sum_\nu \Theta(\epsilon^\nu-V_m)T(\epsilon^\nu), \quad (14)$$

with $I_z=\int d\vec{r}_\perp \vec{j}_z(\vec{r})$. Further, $T(\epsilon)=|[\tilde{\mathbf{S}}(\epsilon)]_{12}|^2=|[\tilde{\mathbf{S}}(\epsilon)]_{21}|^2$, where $\tilde{\mathbf{S}}=\mathbf{k}_\nu^{1/2}\mathbf{S}\mathbf{k}_\nu^{-1/2}$ is the current transmission matrix for the νth channel and $(\mathbf{k}_\nu)_{s,s'}=\delta_{s,s'}k_{s\nu}$. The Θ function serves to remove the channels with exponentially decaying wave functions in the contacts.

In the linear response regime ($V_{\rm SD}\to0, V_1=V_2\equiv0$) and for low temperatures ($T\to0$) we obtain[19] from Eq. (14)

$$G=\frac{2e^2}{h}\sum_\nu^\infty T(E_F-E_\perp^\nu). \quad (15)$$

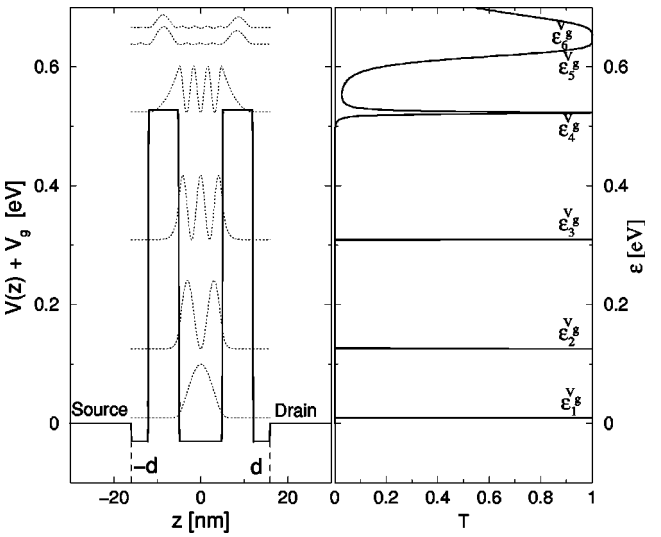

FIG. 2. Left side: Variation of the total potential of our double-barrier test structure. The range of the source- and the drain contact is given by $z<-d$ and $z>d$, respectively. The potential steps of height V_g (which is negative) at $|z|=d$ ($d=16$ nm) result from the voltage applied to the plunger gate. In dotted lines the wave functions $|\psi^{(1)}|^2$ at the resonant energies $\epsilon_i^{V_g}$, $i=1,\ldots,6$ which are the positions of the transmission maxima calculated for the potential $V(z)+V_g$. Right side: Transmission $T(\epsilon)$ as a function of energy for the potential $V(z)+V_g$.

It is seen that the conductance is the superposition of curves $T(E_F-E_\perp^\nu)$ in which the ν dependence only results in an energy shift by $E_\perp^\nu$. $T(\epsilon)$ is determined solely by the one-dimensional scattering problem Eq. (6). Its general features are well known[20] and illustrated in Fig. 2: For small ϵ the transmission is generally small and may have some isolated peaks at ϵ_i. For $\epsilon\sim V_{\rm max}$, where $V_{\rm max}$ is the maximum of $V(z)$, the transmission increases strongly to approach unity for larger energies. Generally, to each resonance a pair index (ν,i) can be assigned, where ν is the channel index and i the number of the maximum in the curve $T(\epsilon)$. As will be shown in the next section, each factor $T(E_F-E_\perp^\nu)$ results from a *coherent* superposition of contributions of resonances with the same channel index ν but with different indices i. In the result we will obtain Fano resonances in T. In each curve $T(E_F-E_\perp^\nu)$ the absolute square has been taken. Therefore the sum in Eq. (15) represents an incoherent superposition of contributions stemming from different classes of resonances. Each class is characterized by the channel index ν.

In the experiments G and therefore T is probed at different energies by varying the voltage of an additional plunger gate. In the case of lateral tunneling this additional gate is a top gate[9,21] and in the case of vertical tunneling it is a side gate.[22] As described in Appendix A we use the following idealization for the total potential in presence of a varying gate voltage: The external potential created by the charges at the gate is screened out completely in the metallic contacts ($|z|>d$) so that the total potential and E_F remain unchanged. In the scattering area ($|z|<d$) the total potential can be idealized for small variations of the gate voltage as a varying potential offset V_g so that $V(z)\to V(z)+V_g$ (see Fig. 2). In Appendix

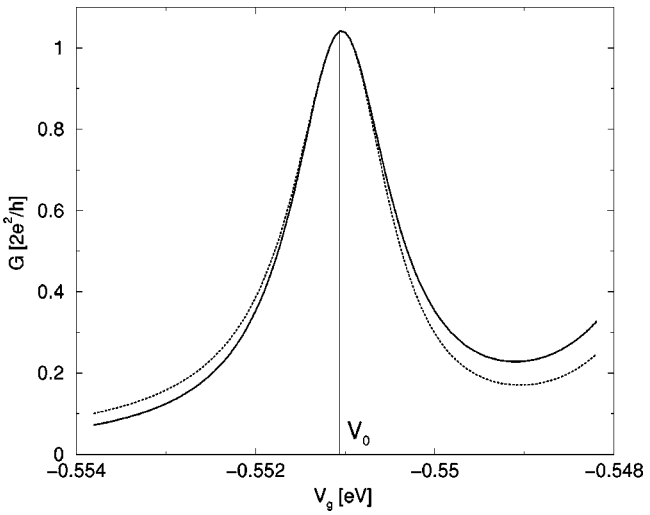

FIG. 3. The conductance as a function of the gate potential V_g around the maximum $i=4$ in Fig. 2; complete calculation (solid line) and approximative values (dotted line) given by Eqs. (15) and (16), respectively. At the maximum the coherent part of the conductance is $G_C(V_0)=2e^2/h$ and the noncoherent part $G_{NC}(V_0) \simeq 0.08\, e^2/h$

A it is shown that in a small domain of gate voltages, $V_g = \delta V + V_0$, around a conductance maximum at $V_g = V_0$ we can write

$$G(V_g) \simeq \frac{2e^2}{h} \sum_{\nu} T^{V_0}(E_F - E_\perp^\nu - \delta V). \tag{16}$$

Here $T^{V_0}(\epsilon)$ is the energy dependent transmission of the structure calculated with the potential $V(z)+V_0$ and $G(V_g)$ is the conductance at V_g. In Fig. 3 it is shown that the relation (16) provides a good approximation for the conductance peak if the resonance is not too broad.

We can assign to each peak in the curve $G(V_g)$ the resonance index (ν_0, i_0) by equating

$$\epsilon_{i_0}^{V_0} = E_F - E_\perp^{\nu_0}, \tag{17}$$

where $V_g = V_0$ is the location of the conductance maximum and $\epsilon_{i_0}^{V_0}$ is the energy of the i_0th maximum of the curve $T^{V_0}(\epsilon)$. If the conductance peak is narrow the resonances with $\nu \neq \nu_0$ provide a slowly varying noncoherent conductivity underground

$$G_{NC} = \frac{2e^2}{h} \sum_{\nu \neq \nu_0} T^{V_0}(E_F - E_\perp^\nu - \delta V). \tag{18}$$

in which the absolute squares of the transmission coefficients are added without phase information. The resonant channel produces a coherent contribution

$$G_C = \frac{2e^2}{h} T^{V_0}(E_F - E_\perp^{\nu_0} - \delta V), \tag{19}$$

which is a coherent superposition of resonances with indices (ν_0, i). In the case of a narrow conductance peak the resonances with $(\nu_0, i \neq i_0)$ constitute a background conductivity

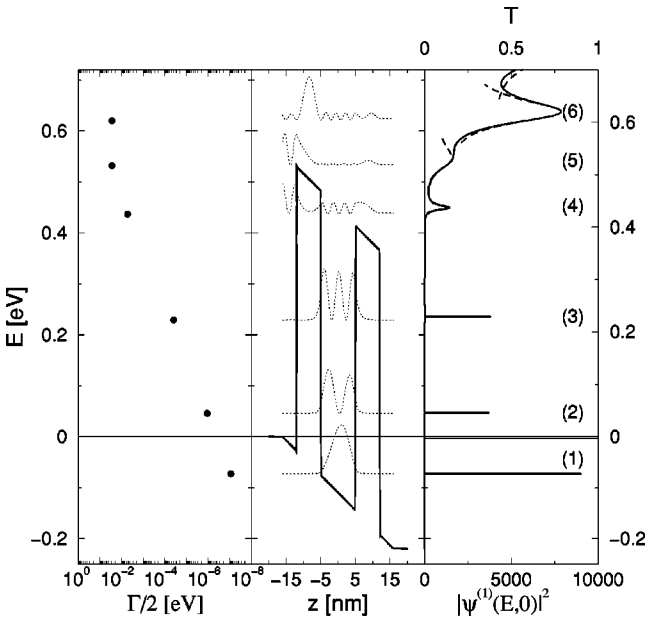

FIG. 4. Middle: Assumed potential in a schematic plot (solid line), wave functions $|\Psi^{(1)}|^2$ at the transmission maxima (dotted line). Right: Transmission vs energy from exact calculation (solid line) and approximation in Eq. (39) (dashed line). Left: Position of the poles of the S matrix in the complex energy plane determined after Eqs. (35) and (36).

as well. However, this background adds coherently to the S matrix as in Eq. (1) leading to Fano profiles. This is in contrast to the noncoherent conductivity background from Eq. (18). We find that in our single-channel coherent transport model a coherent and a noncoherent background conductivity to a transport resonance may coexist.

III. COHERENT CONTRIBUTION TO THE CONDUCTANCE

In the following we are interested in the analysis of narrow transport-resonances. They occur in the resonant part G_c of the conductance as given by Eq. (19). For illustrative purposes and to check our analytical theory we consider $T(\epsilon)$ for the double barrier system of Fig. 2 with an applied source-drain voltage V_{SD}, as depicted in Fig. 4 for $V_{SD} = 220$ meV. In the structure of Fig. 4 the barriers are high enough so that the lowest three quasibound resonances (1–3) and the above lying Fowler-Nordheim-type resonance 4 are narrow and have a little interaction. However, the approximation technique described below gives a very good description of the higher Fabry-Perot-type resonances (5 and 6) in the classically allowed transport regime as well. These resonances have a sizable larger overlap.

A. *R* matrix representation of the *S* matrix

Our theoretical development starts with an R matrix representation of the S matrix which is particularly well suited to the description of narrow resonances. As shown in Refs. 19 the wave functions for the one dimensional problem in Eq. (6) can be written as

$$\psi(\epsilon,z)=R(\epsilon,z,d)\psi^S(\epsilon,d)+R(\epsilon,z,-d)\psi^S(\epsilon,-d), \tag{20}$$

where

$$\psi^S(\epsilon,\pm d)=\pm\frac{1}{m^*}\frac{d\psi}{dz}\bigg|_{z=\pm d}, \tag{21}$$

and $R(\epsilon,z,z')$ is the R matrix. For the points on the 0d surface of the scattering area ($z=\pm d$) we therefore obtain the condition

$$\begin{pmatrix}\psi(-d)\\ \psi(+d)\end{pmatrix}=\begin{pmatrix}R(\epsilon,-d,-d) & R(\epsilon,d,-d)\\ R(\epsilon,-d,d) & R(\epsilon,d,d)\end{pmatrix}\begin{pmatrix}\psi^S(-d)\\ \psi^S(+d)\end{pmatrix}. \tag{22}$$

Using the continuity of the wave functions $\psi=\psi^{\rm in}+\psi^{\rm out}$ and their derivatives at $z=\pm d$ as well as the defining relations (11) and (22) we find that the S and the R matrix are related through

$$\tilde{\mathbf{S}}=\mathbf{k}^{1/2}\mathbf{S}\mathbf{k}^{-1/2}=\mathbf{1}-2[\mathbf{1}+i\mathbf{\Omega}]^{-1}. \tag{23}$$

Here, for each energy $\epsilon=\epsilon^\nu$ we find $(\mathbf{k})_{ss'}=k_{s\nu}\delta_{ss'}$ and the matrix $\mathbf{\Omega}$ of rank two is defined as

$$\mathbf{\Omega}=\mathbf{k}^{1/2}\mathbf{R}\mathbf{k}^{1/2}=\sum_{l=1}^{\infty}\frac{\boldsymbol{\omega}_l}{\epsilon^\nu-\epsilon_l}, \tag{24}$$

with

$$(\boldsymbol{\omega}_l)_{ss'}=\frac{\hbar^2}{2m^*}k_{s\nu}^{1/2}k_{s'\nu}^{1/2}\chi_l[(-1)^s d]\chi_l[(-1)^{s'}d]. \tag{25}$$

The real Wigner-Eisenbud functions χ_l in Eq. (25) are the solutions to the 1D Schrödinger equation

$$\left\{-\frac{\hbar^2}{2m^*}\frac{d^2}{dz^2}+V(z)-\epsilon_l\right\}\chi_l(z)=0, \tag{26}$$

with the boundary conditions $[d\chi_l/dz](z=\pm d)=0$. From Eq. (23) the unitarity of the $\tilde{\mathbf{S}}$ matrix

$$\tilde{\mathbf{S}}\tilde{\mathbf{S}}^\dagger=\tilde{\mathbf{S}}^\dagger\tilde{\mathbf{S}}=\mathbf{1}, \tag{27}$$

is obtained immediately for all real values of ϵ^ν. Due to the special form of the potential the current is conserved in each channel ν.

B. Pole analysis

The starting point for our pole analysis is the following exact reformulation of Eq. (23) in each interval $(\epsilon_{\lambda-1},\epsilon_{\lambda+1}),\lambda\geqslant 1$ (see Appendix B)

$$\tilde{\mathbf{S}}(\epsilon)=\frac{\mathbf{Z}_\lambda(\epsilon)}{\epsilon-\epsilon_\lambda-\overline{\mathcal{E}_\lambda}(\epsilon)}, \tag{28}$$

with

$$\overline{\mathcal{E}_\lambda}(\epsilon)=-i\,\mathrm{Tr}[\boldsymbol{\omega}_\lambda(\mathbf{1}+i\mathbf{\Omega}_\lambda)^{-1}], \tag{29}$$

and the regular matrix

$$\mathbf{\Omega}_\lambda(\epsilon)=\sum_{\substack{n=1\\ n\neq\lambda}}^{\infty}\frac{\boldsymbol{\omega}_n}{\epsilon-\epsilon_n}. \tag{30}$$

The matrix $\mathbf{Z}_\lambda$ can be written as

$$\mathbf{Z}_\lambda(\epsilon)=\frac{\epsilon-\epsilon_\lambda}{\mathcal{D}_\lambda(\epsilon)}[-1-\det[\mathbf{\Omega}]+i(\mathbf{\Omega}-\mathbf{\Omega}^-)], \tag{31}$$

where

$$\mathcal{D}_\lambda(\epsilon)=\det[\mathbf{1}+i\mathbf{\Omega}_\lambda], \tag{32}$$

$(\mathbf{\Omega}^-)_{11}=(\mathbf{\Omega})_{22}$, $(\mathbf{\Omega}^-)_{22}=(\mathbf{\Omega})_{11}$, and $(\mathbf{\Omega}^-)_{12}=(\mathbf{\Omega}^-)_{21}=-(\mathbf{\Omega})_{12}$.

The matrix $\mathbf{Z}_\lambda$ and the function $\overline{\mathcal{E}_\lambda}$ are related to each other through the unitarity requirement for the S matrix which gives

$$\mathbf{Z}_\lambda\mathbf{Z}_\lambda^\dagger=\mathbf{Z}_\lambda^\dagger\mathbf{Z}_\lambda=|\epsilon-\epsilon_\lambda-\overline{\mathcal{E}_\lambda}(\epsilon)|^2. \tag{33}$$

The representation of the S matrix in Eq. (28) has the advantage that it directly yields the equation

$$\epsilon_0-i\Gamma/2-\epsilon_\lambda-\overline{\mathcal{E}_\lambda}(\epsilon_0-i\Gamma/2)=0. \tag{34}$$

to determine the positions $\overline{\epsilon_0}=\epsilon_0-i\Gamma/2$ of the poles in the complex plane. We are interested in narrow resonances for which Γ is a small quantity. We therefore require as the basic assumption for our theory the validity of the linearization of $\overline{\mathcal{E}_\lambda}$ and implicitly $\mathbf{Z}_\lambda$ in a domain of the complex energy plane that includes the pole $\overline{\epsilon_0}$ and the part of the real axis which contains the transmission peak associated with the resonance.

After a first order expansion of $\overline{\mathcal{E}_\lambda}(\epsilon_0-i\Gamma/2)$ around ϵ_0 one obtains from Eq. (34)

$$\epsilon_0=\epsilon_\lambda+\mathcal{E}_1(\epsilon_0)-\frac{\Gamma}{2}\frac{d\mathcal{E}_2}{d\epsilon}\bigg|_{\epsilon=\epsilon_0}, \tag{35}$$

as well as

$$\Gamma=2\mathcal{E}_2(\epsilon_0)\left(1-\frac{d\mathcal{E}_1}{d\epsilon}\bigg|_{\epsilon=\epsilon_0}\right)^{-1}, \tag{36}$$

where $\mathcal{E}_1(\epsilon)=\mathrm{Re}[\overline{\mathcal{E}_\lambda}(\epsilon)]$ and $\mathcal{E}_2(\epsilon)=-\mathrm{Im}[\overline{\mathcal{E}_\lambda}(\epsilon)]$. Equation (35) with Eq. (36) inserted is a nonlinear equation with a unique root for ϵ_0. In Fig. 5(b) it is demonstrated that the resonance energies of the lowest levels are very well represented by our linear approximation.

In principle, if $\mathcal{D}_\lambda(\epsilon)=0$ the $\tilde{\mathbf{S}}$ matrix can have other poles than the ones described in Eq. (34). However, since $\mathcal{D}_\lambda(\epsilon)$ depends only through the regular and slowly varying function $\mathbf{\Omega}_\lambda$ on the energy the complex energy of the poles is expected to have a large imaginary part.

To obtain the line shape of the resonance we employ a formal expansion of the S matrix as given in Eq. (28) in a Laurent series around the pole. Here Eq. (28) ensures that the

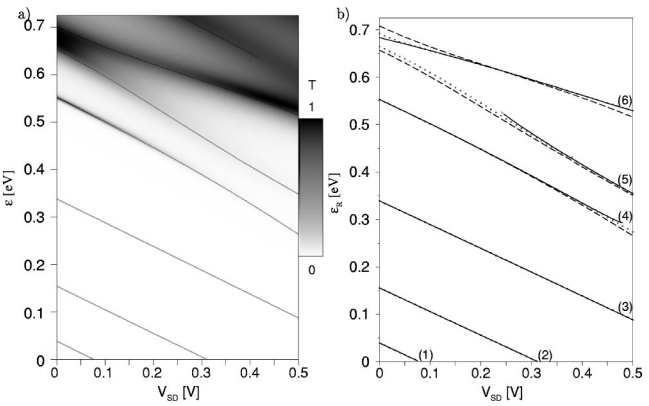

FIG. 5. (a) Transmission as a function of V_{SD} and the kinetic energy ϵ. (b) Energy of maximum transmission vs V_{SD}: Complete calculation (solid lines), result from Eqs. (35) and (36) (dashed lines), and values obtained if the derivatives occurring in Eqs. (35) and (36) are neglected (dotted line). The three lines coincide for the lowest three resonances.

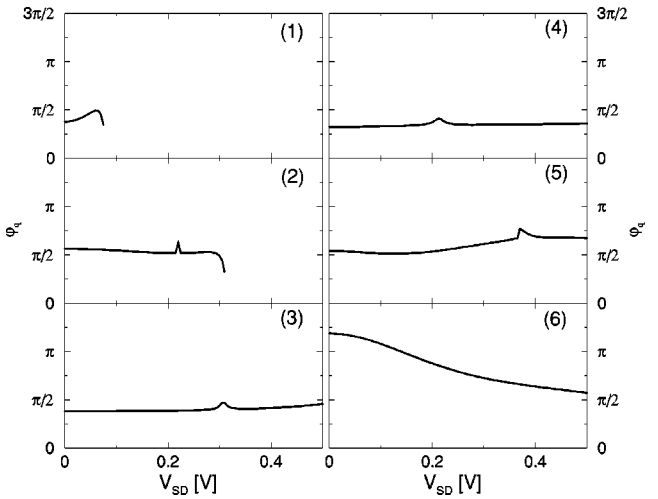

FIG. 6. The argument of the complex asymmetry parameter q vs applied bias. Even for the narrow transmission peaks corresponding to the quasibound states the imaginary part of q is big and thus important for the description of the line shape.

S matrix is an analytic function which is required for the existence of the Laurent series. After the linearization of $\overline{\mathcal{E}_\lambda}$ and $\mathbf{Z}_\lambda$ we obtain (see Appendix C)

$$\tilde{\mathbf{S}}(\epsilon) \simeq i \frac{\tilde{\mathbf{S}}(\epsilon_0) - \tilde{\mathbf{S}}_{\mathrm{bg}}}{e+i} + \tilde{\mathbf{S}}_{\mathrm{bg}}, \tag{37}$$

with

$$\tilde{\mathbf{S}}_{\mathrm{bg}} = \frac{i\Gamma/2}{\epsilon_0 - \epsilon_\lambda - \overline{\mathcal{E}_\lambda}(\epsilon_0)} \frac{d\mathbf{Z}_\lambda}{d\epsilon}\bigg|_{\epsilon=\epsilon_0}, \tag{38}$$

where $e = 2(\epsilon - \epsilon_0)/\Gamma$. Equation (37) has the general form of Eq. (1), where we can provide an explicit expression for $\tilde{\mathbf{S}}_{\mathrm{bg}}$. From Eq. (37) a line shape

$$T(\epsilon) = |[\tilde{\mathbf{S}}(\epsilon)]_{12}|^2 = T_{\mathrm{bg}} \frac{[e + \mathrm{Re}(q)]^2 + [\mathrm{Im}(q)]^2}{e^2+1} \tag{39}$$

is deduced where $T_{\mathrm{bg}} = |(\tilde{\mathbf{S}}_{\mathrm{bg}})_{12}|^2$ is the background transmission. The right-hand side of Eq. (39) is a Fano distribution with a complex asymmetry parameter q given by

$$q = i[\tilde{\mathbf{S}}(\epsilon_0)]_{12} (\tilde{\mathbf{S}}_{\mathrm{bg}})^{-1}_{12}. \tag{40}$$

The numerical calculations in Fig. 6 confirm that a complex asymmetry parameter is the general finding. This seems to hold for narrow peaks as well as for broad and overlapping peaks.

On the background of our systematic pole analysis we want to discuss a common practice in which an ansatz for the S matrix of the form of Eq. (37) with general $\tilde{\mathbf{S}}_{\mathrm{bg}}$ and $\tilde{\mathbf{S}}(\epsilon_0)$ is made.[12–14] To restrict this ansatz to physically meaningful cases the unitarity of $\tilde{\mathbf{S}}$ is generally required for *all* real energies. In Appendix D it is shown that in this case the asymmetry parameter q_r is real and that $\tilde{\mathbf{S}}_{\mathrm{bg}}$ has only one real free parameter which can be chosen to be q_r. In our opinion, this requirement is an overconstraint since the objective is a good description of the main part of the transmission peak up to energies of about $e \approx 1$. Our pole analysis provides a systematic description of the line shape in this energy range. The resulting expression (37) preserves the unitarity of the scattering matrix only in linear order e (see Appendix D):

$$\tilde{\mathbf{S}}\tilde{\mathbf{S}}^\dagger = \tilde{\mathbf{S}}^\dagger\tilde{\mathbf{S}} \simeq \mathbf{1} + (\boldsymbol{\delta} - \mathbf{1}) \frac{e^2}{e^2+1}. \tag{41}$$

The background matrix $\tilde{\mathbf{S}}_{\mathrm{bg}}$ is then characterized by three parameters. They can be chosen as the real and the imaginary part of the complex asymmetry parameter q given by Eqs. (38) and (40) and the imaginary part of the complex asymmetry parameter q_R describing the line shape of the resonance in reflection. As shown in Fig. 7 the matrix elements of $\boldsymbol{\delta} - \mathbf{1}$ are small in comparison with 1. We expect that our

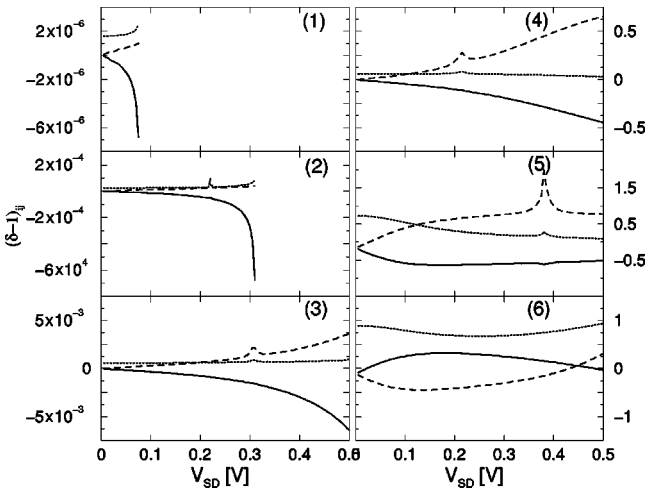

FIG. 7. The deviation from the unitarity of the $\tilde{\mathbf{S}}$-matrix given by the approximative expression (37): $\hat{\delta}_{11} - 1$ (solid line), $\hat{\delta}_{22} - 1$ (dashed line), and $|\hat{\delta}_{12}|$ (dotted line) as a function of applied bias.

approximation is valid as long as the second term on the right hand side of Eq. (41) is small compared to 1. Then the deviation of $\tilde{\mathbf{S}}$ from unitarity is small. This way, for each maximum we can estimate the range of validity for our approximation through the requirement $(\boldsymbol{\delta}-\mathbf{1})_{ij}e^2/(e^2+1) \ll 1, i,j=1,2$.

C. Coherent conductance

Inserting Eq. (39) in (19) we obtain the coherent contribution to the conductance in the vicinity of the resonance as a Fano function with the complex asymmetry parameter q defined by Eq. (40),

$$G_{\mathrm{C}}=G_{\mathrm{C}}^{\mathrm{bg}}\frac{[\tilde{e}+\mathrm{Re}(q)]^2+[\mathrm{Im}(q)]^2}{\tilde{e}^2+1}. \tag{42}$$

Here $\tilde{e}=2(V_g-V_0)/\Gamma$ is a function of the plunger gate potential V_g, the resonance position V_0 and the resonance width Γ. The background coherent contribution is related to the background transmission through

$$G_{\mathrm{C}}^{\mathrm{bg}}=\frac{2e^2}{h}T_{\mathrm{bg}}. \tag{43}$$

The behavior of the systems analyzed in this paper [Eq. (42)] shows that an asymmetric line shape arises in general when there is a coherent superposition of contributions to the S matrix coming from different poles. This does not necessarily involve the coupling between two different channels as in the usual scenario to explain Fano resonances.

IV. DISCUSSION

After having evaluated the resonant part we obtain for the total conductance

$$G=G_{\mathrm{NC}}^{\mathrm{bg}}+G_{\mathrm{C}}^{\mathrm{bg}}\frac{[\tilde{e}+\mathrm{Re}(q)]^2+[\mathrm{Im}(q)]^2}{\tilde{e}^2+1}. \tag{44}$$

Here we assumed a small overlap of the conductance peaks so that the contribution of the nonresonant channels can be approximated by a constant

$$G_{\mathrm{NC}}^{\mathrm{bg}}=\frac{2e^2}{h}\sum_{\nu\neq\nu_0}^{\infty}T^{V_0}(E_F-E_\perp^\nu). \tag{45}$$

In our theory all parameters in Eq. (44) can be calculated microscopically.

Now we solve the inverse problem to extract the transmission through the resonant channel ν_0 from the experimental conductance data. Here we face the basic problem that the parameters q, $G_{\mathrm{C}}^{\mathrm{bg}}$, V_0, and Γ needed to apply Eq. (39) cannot be gained from a fit in a unique way. To see this we rewrite Eq. (44) in an equivalent form[10]

$$G=G_{\mathrm{of}}+G_0\frac{[\tilde{e}+q_F]^2}{\tilde{e}^2+1}. \tag{46}$$

This is a sum of a Fano line with a real asymmetry parameter

$$q_F=[|q|^2-1+\sqrt{(|q|^2-1)^2+4(\mathrm{Re}\,q)^2}]/2\,\mathrm{Re}\,q, \tag{47}$$

and a constant offset

$$G_{\mathrm{of}}=G_{\mathrm{NC}}^{\mathrm{bg}}+G_{\mathrm{C}}^{\mathrm{bg}}-G_0, \tag{48}$$

where

$$G_0=G_{\mathrm{C}}^{\mathrm{bg}}\frac{\mathrm{Re}\,q}{q_F}. \tag{49}$$

The parameter q_F is obtained as a solution of a second order equation where we choose the value which leads to a positive G_0. The other choice for the sign in q_F yields an equivalent description. According to Eq. (46) a fit of the conductance line shape near a resonance can fix only the real parameters G_{of}, G_0, q_F, V_0, and Γ which are not enough for a unique separation of the coherent from the noncoherent part of the conductance. In order to define a bijective mapping of the set of the five fitting parameters onto the microscopic parameter set $G_{\mathrm{NC}}^{\mathrm{bg}}$, $G_{\mathrm{C}}^{\mathrm{bg}}$, $\mathrm{Re}(q)$, $\mathrm{Im}(q)$, V_0, and Γ, we need a supplemental variable which we call α. We observe that the equivalence of the two conductance expressions (44) and (46) allows the variation of the background components of the conductance only inside a small domain: From Eqs. (47) and (49) it follows that $G_{\mathrm{C}}^{\mathrm{bg}}\geqslant G_0$. Taking into account that $G_{\mathrm{NC}}^{\mathrm{bg}}$ is per construction positive it immediately results from Eq. (48) that $G_{\mathrm{C}}^{\mathrm{bg}}\leqslant G_0+G_{\mathrm{of}}$. Thus we can define the parameter α as

$$G_{\mathrm{C}}^{\mathrm{bg}}=G_0+\alpha G_{\mathrm{of}} \tag{50}$$

where α varies between zero and one. The complex asymmetry parameter and the noncoherent background component of the conductance can be expressed as a function of α as well:

$$\mathrm{Re}(q)=q_F\frac{G_0}{G_0+\alpha G_{\mathrm{of}}}, \tag{51}$$

$$\mathrm{Im}(q)=\frac{G_{\mathrm{of}}}{G_0+\alpha G_{\mathrm{of}}}\sqrt{\alpha^2+(1+q_F^2)\,\alpha\,\frac{G_0}{G_{\mathrm{of}}}}, \tag{52}$$

and

$$G_{\mathrm{NC}}^{\mathrm{bg}}=(1-\alpha)G_{\mathrm{of}}. \tag{53}$$

Using the values V_0 and Γ from fitting and the expressions (50)–(52) it is very easy to construct the off-diagonal part of the S matrix associated with the resonant channel ν_0 up to a global phase factor. This missing phase factor is expected because the absolute square has been taken in Eq. (39).

Using the expression (44) we have performed an analysis of the experimental conductance data in the Fano regime published by Göres *et al.*[9] We include a possible constant component due to incoherent transport (G_{inc} in Ref. 9) in an effective noncoherent conductance background. In the experimental system the potential in the plane of the two-dimensional electron gas is not known in detail. The two major reasons are, first, the complexity of the geometry of the top gate electrodes. Second, experimentally the potential

changes in an unpredictable way if the sample is heated and then cooled down again.[9] These changes are attributed to unknown metastabilities of electrons in the donor layer within the AlGaAs. Without sufficient knowledge of the electron potential it is clear that it is impossible to calculate the conductance exactly. Instead, we assume the correctness of a simple ansatz for the potential. We then focus on the question what can be learned from the experimental peaks about the pole structure of the S matrix which describes the resonance theoretically. As an ansatz for the potential we choose the effectively one-dimensional model presented in Sec. II [see Eq. (3)]. One reason for picking this model is that we can carry out an analytical analysis of the pole structure of the S matrix which is independent of the particular shape of $V(z)$ and $V(\vec{r}_\perp)$ (see Sec. III). Second, we adopt the discussion in Sec. II of Ref. 23 to argue that our model is suitable for the representation of the relevant part of the experimental structure: As shown in Fig. 3 of this reference, the scattering states are formed in the contacts which are widening into the reservoir. With the reservoir we associate the semi-infinite two-dimensional electron gases on the source and on the drain side of the quantum dot presented in Fig. 1 of Ref. 9. The reservoirs have a low resistivity. With the contacts shown in Fig. 3 of Ref. 23 we associate the constrictions in the experimental samples between two split gates denoted by I in Fig. 1 of Ref. 9. In our model the contacts have to be identified with the regions denoted with "1d" in Fig. 1 of this paper which lie between the reservoirs (source and drain) and the barrier. In our simple model we neglect interactions between the one-dimensional channels in the contacts. In reality this scattering is expected to have a significant impact. It is, however, plausible to assume in this first study that the conductance will have the same form and only the microscopic definitions of the parameters are modified by the new interaction. As a consequence it is to be expected that under inclusion of channel scattering the asymmetry parameter q_F can vary in a wider range from zero for the symmetrical dip of an antiresonance to infinity for a Breit-Wigner profile. In the case of decoupled channels we only find large values of q_F which correspond to maxima in the conductance.

Underlying our method we find for the first antiresonance presented in Fig. 2(a) of Ref. 9 that the offset conductance is not only generated by the incoherent processes as it is proposed there. Rather, from Eq. (50) it follows that the coherent contribution to the background conductance should have a value between 0.131 e^2/h and 0.210 e^2/h while the noncoherent background part $G_{\mathrm{NC}}^{\mathrm{bg}}$ varies from 0 to 0.210 e^2/h. We conclude that the offset term G_{inc} given by Göres *et al.*[9] in Eq. (3) in general represents a number of different components which can be coherent or noncoherent.

From the experimental conductance data we can also extract the transmission curve $T(\epsilon)$ as used in Eq. (15) in the vicinity of a resonance and verify that the energy dependence is given by a Fano function with a complex asymmetry parameter. For the case analyzed in Fig. 8 the line shape is a typical antiresonance ($q_F = -0.06$). This demonstrates that the existence of many poles in the S matrix leads to an asymmetry of the profile as we have shown in Sec. III and that the channel coupling increases the asymmetry.

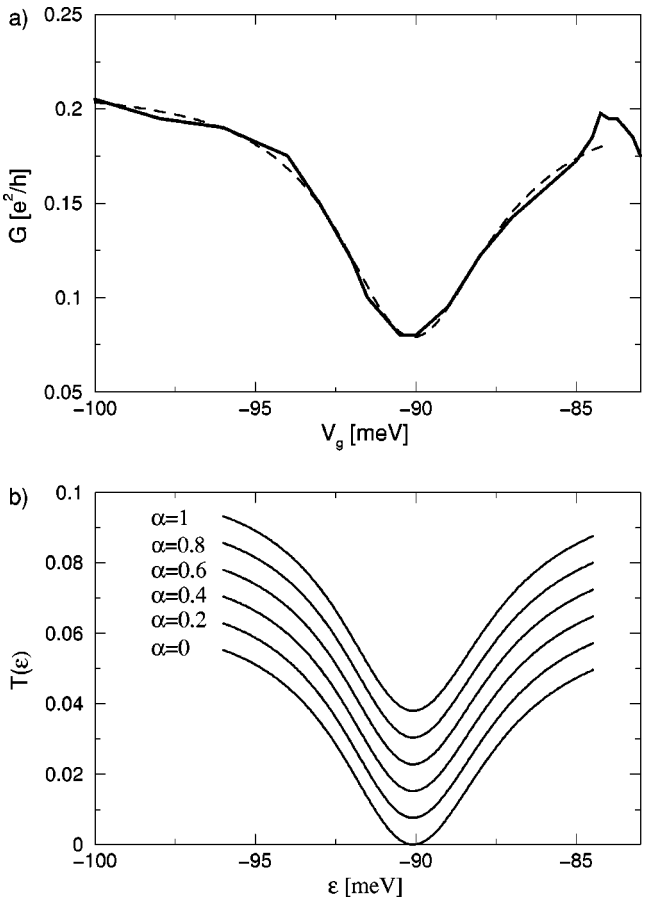

FIG. 8. (a) Conductance as a function of the plunger gate potential V_g: experimental curve from Ref. 9 (solid line) and theoretical calculation (dashed line) using Eq. (46). The parameters of the theoretical curve are $V_0 = -90.24$ meV, $\Gamma = 5.76$ meV, $q_F = -0.054$, $G_0 = 0.131 e^2/h$, and $G_{\mathrm{of}} = 0.079 e^2/h$. (b) The transmission through the resonant channel ν_0 as a function of energy for a few values of α.

V. SUMMARY

We have provided in this paper a systematic treatment of the conductance through a quantum dot embedded in a quantum wire. In our system the potential is decoupled in the transport and in the lateral direction which means that the scattering channels are also decoupled. The Fano function with a complex asymmetry parameter arises as the most general resonance line shape under the assumption that the background can be considered constant over the width of the resonance. Our model provides microscopic expressions for the line shape parameters and predicts the coherent and noncoherent contributions to the background conductance. Also this method allows the reconstruction of the off-diagonal part in the scattering matrix from the experimental conductance data and shows that other measurements are necessary to determine the S matrix in an unique way.

APPENDIX A: MODEL FOR THE PLUNGER GATE

Following Eq. (26) the Wigner-Eisenbud functions χ_l are then unchanged and the Wigner-Eisenbud energies become $\epsilon_l \to \epsilon_l + V_g$. We define for the linear response regime $V_1 = V_2 = 0$ and $k(\epsilon^\nu) = k_{1\nu} = k_{2\nu}$. Then, according to Eq. (25) the matrices $\boldsymbol{\omega}_l$ are independent of V_g. We now consider a small voltage domain $V_g = V_0 + \delta V$ around the conductance maximum in which the sharp resonance extends. It then follows from Eqs. (24) and (25)

$$
\begin{aligned}
(\boldsymbol{\Omega}^{V_g})_{ss'}(\epsilon^\nu) &= \sum_{l=1}^{\infty} \frac{[\boldsymbol{\omega}_l(\epsilon)]_{ss'}}{\epsilon^\nu - \epsilon_l - V_g} \\
&= \frac{\hbar^2}{2m^*} k(\epsilon^\nu) \sum_{l=1}^{\infty} \frac{\chi_l[(-1)^s d]\chi_l[(-1)^{s'} d]}{\epsilon^\nu - \epsilon_l - V_0 - \delta V} \\
&\approx \frac{\hbar^2}{2m^*} k(\epsilon^\nu - \delta V) \\
&\quad \times \sum_{l=1}^{\infty} \frac{\chi_l[(-1)^s d]\chi_l[(-1)^{s'} d]}{(\epsilon^\nu - \delta V) - \epsilon_l - V_0} \\
&= (\boldsymbol{\Omega}^{V_0})_{ss'}(\epsilon^\nu - \delta V), \qquad \text{(A1)}
\end{aligned}
$$

where $\boldsymbol{\Omega}^{V_g}$ is the matrix $\boldsymbol{\Omega}$ with allied potential shift V_g. From Eq. (A1) it can be gathered that as long as we can approximate in the slowly varying function $k(\epsilon^\nu) \approx k(\epsilon^\nu - \delta V)$ the gate-voltage dependence of $\boldsymbol{\Omega}$ can be absorbed in a simple shift of the energy argument of $\boldsymbol{\Omega}$ at constant gate voltage. From Eqs. (23) and (A1) we obtain $\tilde{\mathbf{S}}^{V_g}(\epsilon^\nu) \approx \tilde{\mathbf{S}}^{V_0}(\epsilon^\nu - \delta V)$ and therefore

$$
T^{V_g}(E_F - E_\perp^\nu) \approx T^{V_0}(E_F - E_\perp^\nu - \delta V). \qquad \text{(A2)}
$$

APPENDIX B: $\tilde{\mathbf{S}}$ MATRIX

In order to express the $\tilde{\mathbf{S}}$ matrix given by Eq. (23) in terms of $\boldsymbol{\Omega}_\lambda$ and $\boldsymbol{\omega}_\lambda$ for all energies in $(\epsilon_{\lambda-1}, \epsilon_{\lambda+1})$ we have to invert the matrix

$$
\begin{aligned}
\mathbf{1} + i\boldsymbol{\Omega} &= \mathbf{1} + i\boldsymbol{\Omega}_\lambda + \frac{i\boldsymbol{\omega}_\lambda}{\epsilon - \epsilon_\lambda} \\
&= [\mathbf{1}(\epsilon - \epsilon_\lambda) \\
&\quad + i\boldsymbol{\omega}_\lambda (\mathbf{1} + i\boldsymbol{\Omega}_\lambda)^{-1}] \frac{\mathbf{1} + i\boldsymbol{\Omega}_\lambda}{\epsilon - \epsilon_\lambda}. \qquad \text{(B1)}
\end{aligned}
$$

It results immediately

$$
\det[\mathbf{1} + i\boldsymbol{\Omega}] = \frac{\epsilon - \epsilon_\lambda - \bar{\mathcal{E}}_\lambda(\epsilon)}{\epsilon - \epsilon_\lambda} \mathcal{D}_\lambda(\epsilon) \qquad \text{(B2)}
$$

with $\bar{\mathcal{E}}_\lambda(\epsilon)$ and $\mathcal{D}_\lambda(\epsilon)$ defined in Eqs. (29) and (32), respectively. The scattering matrix becomes

$$
\tilde{\mathbf{S}}(\epsilon) = \mathbf{1} - 2\frac{(\mathbf{1} + i\boldsymbol{\Omega}_\lambda)^{-1}(\epsilon - \epsilon_\lambda) + i\boldsymbol{\omega}_\lambda^- / \mathcal{D}_\lambda(\epsilon)}{\epsilon - \epsilon_\lambda - \bar{\mathcal{E}}_\lambda(\epsilon)}, \qquad \text{(B3)}
$$

where $\boldsymbol{\omega}_\lambda^-$ is defined as $\boldsymbol{\Omega}^-$. We identify the denominator function of the above expression of $\tilde{\mathbf{S}}$ with $\mathbf{Z}_\lambda(\epsilon)$ used in Eq. (28).

APPENDIX C: LAURENT EXPANSION OF $\tilde{\mathbf{S}}$ AROUND A POLE

We associate each resonance with a single pole $\bar{\epsilon}_0 = \epsilon_0 - i\Gamma/2$ in the $\tilde{\mathbf{S}}(\epsilon)$ and perform formally a Laurent expansion of this matrix around the pole:

$$
\tilde{\mathbf{S}}(\bar{\epsilon}) = \frac{\mathbf{A}_{-1}}{\epsilon - \epsilon_0 + i\Gamma/2} + \mathbf{A}_0 + \sum_{j=1}^{\infty} \mathbf{A}_j (\bar{\epsilon} - \epsilon_0 + i\Gamma/2)^j. \qquad \text{(C1)}
$$

We have defined the resonance domain as a region in the complex energy plane in the vicinity of $\bar{\epsilon}_0$ which includes at least the interval $(\epsilon_0 - \Gamma/2, \epsilon_0 + \Gamma/2)$ on the real axis and inside which we can linearize $\bar{\mathcal{E}}_\lambda$ and $\mathbf{Z}_\lambda$. Thus the derivatives up to the second order for these two functions at the points $\bar{\epsilon}_0$ and ϵ_0 are very small and we can neglect them in the expression of the expansion coefficients of the Laurent series. In the limits our approximation the coefficients have the form

$$
\mathbf{A}_{-1} \simeq \frac{\mathbf{Z}_\lambda(\epsilon_0) - i\Gamma/2 (d\mathbf{Z}_\lambda/d\epsilon)|_{\epsilon=\epsilon_0}}{1 - d\bar{\mathcal{E}}_\lambda/d\epsilon|_{\epsilon=\epsilon_0}}, \qquad \text{(C2)}
$$

$$
\mathbf{A}_0 \simeq \frac{d\mathbf{Z}_\lambda/d\epsilon|_{\epsilon=\epsilon_0}}{1 - d\bar{\mathcal{E}}_\lambda/d\epsilon|_{\epsilon=\epsilon_0}}, \qquad \text{(C3)}
$$

and $\mathbf{A}_j \simeq 0, \forall j \geqslant 1$. According to Eqs. (35) and (36)

$$
1 - \left.\frac{d\bar{\mathcal{E}}_\lambda}{d\epsilon}\right|_{\epsilon=\epsilon_0} = \frac{\epsilon_0 - \epsilon_\lambda - \bar{\mathcal{E}}_\lambda(\epsilon_0)}{i\Gamma/2} \qquad \text{(C4)}
$$

and $\mathbf{A}_0$ becomes identically with $\tilde{\mathbf{S}}_{\rm bg}$ given by Eq. (38). From this it follows also $\mathbf{A}_{-1} = i[\tilde{\mathbf{S}}(\epsilon_0) - \tilde{\mathbf{S}}_{\rm bg}]\Gamma/2$.

APPENDIX D: UNITARITY OF THE $\tilde{\mathbf{S}}$ MATRIX

From Eq. (37) we obtain for all energies:

$$
\begin{aligned}
\tilde{\mathbf{S}}(\epsilon)\tilde{\mathbf{S}}^\dagger(\epsilon) &\simeq \tilde{\mathbf{S}}_{\rm bg}\tilde{\mathbf{S}}_{\rm bg}^\dagger \frac{e^2}{e^2+1} + \tilde{\mathbf{S}}(\epsilon_0)\tilde{\mathbf{S}}^\dagger(\epsilon_0)\frac{1}{e^2+1} \\
&\quad - i[\tilde{\mathbf{S}}_{\rm bg}\tilde{\mathbf{S}}^\dagger(\epsilon_0) - \tilde{\mathbf{S}}(\epsilon_0)\tilde{\mathbf{S}}_{\rm bg}^\dagger]\frac{e}{e^2+1}, \qquad \text{(D1)}
\end{aligned}
$$

where $e = 2(\epsilon - \epsilon_0)/\Gamma$. Here

$$
\tilde{\mathbf{S}}(\epsilon_0)\tilde{\mathbf{S}}^\dagger(\epsilon_0) = \mathbf{1} \qquad \text{(D2)}
$$

is exactly fulfilled because the linearization is exact at the real energy ϵ_0. Taking into account the definition (38) of $\tilde{\mathbf{S}}_{\rm bg}$ we find the first step in

$$[\tilde{\mathbf{S}}_{\rm bg}\tilde{\mathbf{S}}^{\dagger}(\epsilon_0)-\tilde{\mathbf{S}}(\epsilon_0)\tilde{\mathbf{S}}^{\dagger}_{\rm bg}]=\frac{i\Gamma/2(d/d\epsilon)(\mathbf{Z}_\lambda\mathbf{Z}^{\dagger}_\lambda)|_{\epsilon=\epsilon_0}}{|\epsilon_0-\epsilon_\lambda-\overline{\mathcal{E}_\lambda}(\epsilon_0)|^2}=0, \tag{D3}$$

and the second step is obtained differentiating the relation (33) with respect to the energy. The condition (D3) is sufficient for the unitarity of $\tilde{\mathbf{S}}$ in first order in e. Thus our linearization of $\mathbf{Z}_\lambda$ and $\overline{\mathcal{E}_\lambda}$ leads to a consistent theory.

In general the symmetrical complex matrix $\tilde{\mathbf{S}}_{\rm bg}$ can be written in the form

$$\tilde{\mathbf{S}}_{\rm bg}=\begin{pmatrix} \frac{i}{q_R}[\tilde{\mathbf{S}}(\epsilon_0)]_{11} & \frac{i}{q}[\tilde{\mathbf{S}}(\epsilon_0)]_{12} \\ \frac{i}{q}[\tilde{\mathbf{S}}(\epsilon_0)]_{12} & \frac{i}{q'_R}[\tilde{\mathbf{S}}(\epsilon_0)]_{22} \end{pmatrix} \tag{D4}$$

using the (complex) asymmetry parameters for transmission, q defined in Eq. (40) and for reflection, q_R and q'_R. In the limit of our linear approximation $\tilde{\mathbf{S}}_{\rm bg}$ has to satisfy the Hermitian condition (D3) and thus only three real parameters can be chosen freely, for example, $\mathrm{Im}(1/q_R)$, $\mathrm{Re}(1/q)$, and $\mathrm{Im}(1/q)$:

$$\tilde{\mathbf{S}}_{\rm bg}=\frac{i}{q}\tilde{\mathbf{S}}(\epsilon_0)-\begin{pmatrix} \tau[\tilde{\mathbf{S}}(\epsilon_0)]_{11} & 0 \\ 0 & -\tau^*[\tilde{\mathbf{S}}(\epsilon_0)]_{22} \end{pmatrix}, \tag{D5}$$

with

$$\tau=\mathrm{Im}\left(\frac{1}{q_R}\right)-\mathrm{Im}\left(\frac{1}{q}\right)+\frac{i}{1-T(\epsilon_0)}\mathrm{Re}\left(\frac{1}{q}\right) \tag{D6}$$

and $T(\epsilon_0)$ is the transmission probability at the energy ϵ_0. As can be seen from Eq. (35) ϵ_0 is only an approximative value of the resonance energy so that $T(\epsilon_0)<1$ and τ has no singularity.

Using Eq. (D3) we obtain directly Eq. (41) from Eq. (D1) if we identify the first term on the right-hand side of Eq. (D1) with $\boldsymbol{\delta}e^2/(e^2+1)$ in Eq. (41). Using Eq. (D5) we obtain for the matrix elements of $\boldsymbol{\delta}$

$$\boldsymbol{\delta}_{11}=[1-T(\epsilon_0)]\left|\frac{i}{q}-\tau\right|^2+T(\epsilon_0)\left|\frac{i}{q}\right|^2, \tag{D7}$$

$$\boldsymbol{\delta}_{22}=[1-T(\epsilon_0)]\left|\frac{i}{q^*}-\tau\right|^2+T(\epsilon_0)\left|\frac{i}{q}\right|^2, \tag{D8}$$

$$\boldsymbol{\delta}_{12}=2\tau\mathrm{Im}\left(\frac{1}{q}\right)[\tilde{\mathbf{S}}(\epsilon_0)]_{11}[\tilde{\mathbf{S}}(\epsilon_0)]^*_{12}. \tag{D9}$$

If we artificially impose the unitarity condition on $\tilde{\mathbf{S}}_{\rm bg}$ ($\boldsymbol{\delta}\rightarrow\mathbf{1}$) there remains only one free variable which describes the background matrix. This can be chosen as the real Fano asymmetry parameter denoted with q_r:

$$\tilde{\mathbf{S}}_{\rm bg}=\frac{i}{q_r}\tilde{\mathbf{S}}(\epsilon_0)-\begin{pmatrix} \tau_r[\tilde{\mathbf{S}}(\epsilon_0)]_{11} & 0 \\ 0 & -\tau_r^*[\tilde{\mathbf{S}}(\epsilon_0)]_{22} \end{pmatrix}, \tag{D10}$$

with

$$\tau_r=\frac{1}{1-T(\epsilon_0)}\left[\pm\sqrt{1-T(\epsilon_0)\left(1+\frac{1}{q_r^2}\right)}+\frac{i}{q_r}\right]. \tag{D11}$$

The real parameter q_r should satisfy the inequality $T(\epsilon_0)(1+1/q_r^2)\leqslant 1$.

We can also remark here that assuming in Eq. (1) the background contribution to the S matrix as zero[15] the relation (D1) becomes

$$\tilde{\mathbf{S}}(\epsilon)\tilde{\mathbf{S}}^{\dagger}(\epsilon)=\frac{\mathbf{1}}{e^2+1}. \tag{D12}$$

The unitarity of the scattering matrix (27) restricts strongly $[e^2/(e^2+1)\ll 1]$ the domain inside which the common Wigner-Breit profile yields a good description of the transmission even for extremely narrow and isolated peaks.

*Permanent address: University of Bucharest, Faculty of Physics, PO Box.MG 11, 76900 Bucharest-Magurele, Romania

[1] U. Fano, Phys. Rev. **124**, 1866 (1961).

[2] A. Bohm, *Quantum Mechanics* (Springer, New York, 1993), Chap. 18.

[3] E. Tekman and P. F. Bagwell, Phys. Rev. B **48**, 2553 (1993).

[4] P. F. Bagwell, Phys. Rev. B **41**, 10 354 (1993); C. S. Kim, A. M. Satanin, Y. S. Joe, and R. M. Cosby, *ibid.* **60**, 10 962 (1999); C. S. Kim and A. M. Satanin, Physica E (Amsterdam) **4**, 211 (1999).

[5] R. C. Bowen, W. R. Frensley, G. Klimeck, and R. Lake, Phys. Rev. B **52**, 2754 (1995).

[6] W. Porod, Z. Shao, and C. S. Lent, Phys. Rev. B **48**, 8495 (1993); Z. Shao, W. Porod, and S. Lent, *ibid.* **49**, 7453 (1994); R. Akis, P. Vasilopoulos, and P. Debray, *ibid.* **56**, 9594 (1997); K. Nikolic and R. Sordan, *ibid.* **58**, 9631 (1998); H. Chen and Y. Shi, Phys. Lett. A **262**, 76 (1999); O. A. Tkachenko, V. A. Tkachenko, D. G. Baksheev, and Z. D. Kvon, JETP Lett. **71**, 255 (2000).

[7] A. Yacoby, M. Heiblum, D. Mahalu, and H. Shtrikman, Phys. Rev. Lett. **74**, 4047 (1995); C. Ryu and S. Y. Cho, Phys. Rev. B **58**, 3572 (1998).

[8] J. U. Nöckel and A. D. Stone, Phys. Rev. B **51**, 17 219 (1995).

[9] J. Göres, D. Goldhaber-Gordon, S. Heemeyer, M. A. Kastner, H. Shtrikman, D. Mahalu, and U. Meirav, Phys. Rev. B **62**, 2188 (2000).

[10] G. Abstreiter, M. Cardona, and A. Pinczuk, in *Light Scattering in Solids*, edited by M. Cardona and G. Güntherodt, Topics in Applied Physics Vol. 54 (Springer, Berlin, 1984), p. 127; K. J. Jin, S. H. Pan, and G. Z. Yang, Phys. Rev. B **50**, 8584 (1994).

[11] G. S. Agarwal, S. L. Haan, and J. Cooper, Phys. Rev. A **29**, 2552 (1984).

[12] J. U. Nöckel and A. D. Stone, Phys. Rev. B **50**, 17 415 (1994).
[13] M. Büttiker, Phys. Rev. B **38**, 12 724 (1988).
[14] L. D. Landau and E. M. Lifschitz, *Quantum Mechanics (Non-Relativistic Theory*) (Pergamon, Oxford, 1977), Sec. 145.
[15] Often the background matrix $\tilde{\mathbf{S}}_{bg}$ is assumed to be absent leading to a symmetrical Wigner-Breit shape of the transmission peak (Ref. 16).
[16] Y. Alhassid and H. Attias, Phys. Rev. B **54**, 2696 (1996); Y. Alhassid and H. Attias, Phys. Rev. Lett. **76**, 1711 (1996).
[17] *Mesoscopic Physics and Electronics*, edited by T. Ando, Y. Arakawa, K. Furuya, S. Komiyama, and H. Nakashima (Springer, Berlin, 1998), Chap. 1.6.5.
[18] R. Landauer, IBM J. Res. Dev. **1**, 223 (1957); R. Landauer, Z. Phys. B: Condens. Matter **68**, 217 (1987); D. S. Fisher and P. A. Lee, Phys. Rev. B **23**, 6851 (1981); M. Büttiker, Phys. Rev. Lett. **57**, 1761 (1986); M. Büttiker, IBM J. Res. Dev. **32**, 317 (1988); A. D. Stone and A. Szafer, *ibid.* **32**, 384 (1988); J. Kučera, Czech. J. Phys. **41**, 749 (1991).
[19] L. Smrčka, Supercond. Sci. Technol. **8**, 221 (1990); U. Wulf, J. Kučera, and E. Sigmund, Comput. Mater. Sci. **11**, 117 (1998); U. Wulf, J. Kučera, P. N. Racec, and E. Sigmund, Phys. Rev. B **58**, 16 209 (1998); P. N. Racec, U. Wulf, and J. Kučera, Solid-State Electron. **44**, 881 (2000).
[20] H. Mizuta and T. Tanoue, *The Physics and Applications of Resonant Tunnelling Diodes* (Cambridge University Press, Cambridge, 1995), Chap. 2; C. Presilla and J. Sjöstrand, J. Math. Phys. **37**, 4816 (1996).
[21] M. A. Kastner, Phys. Today **46**, 24 (1993); D. Goldhaber-Gordon, J. Göres, M. A. Kastner, H. Shtrikman, D. Mahalu, and U. Meirav, Phys. Rev. Lett. **81**, 5225 (1998).
[22] S. Tarucha, D. G. Austing, T. Honda, R. J. van der Hage, and L. P. Kouwenhoven, Phys. Rev. Lett. **77**, 3613 (1996).
[23] M. Büttiker, Phys. Rev. B **46**, 12 485 (1992).